Supplementary information
Hepatitis B virus surface antigen drives T-cell immunity through non-canonical antigen presentation in mice

Authors

Xiaofang Li[1,†], Wenxuan Sun[1,†], Xiaolan Xu[1], Qirong Jiang[2], Yuheng Shi[1], Huixi Zhang[1], Weien Yu[2], Bisheng Shi[1], Simin Wan[1], Jiangxia Liu[1], Wuhui Song[1], Jiming Zhang[2], Zhenghong Yuan [1,*] & Jianhua Li[1,*]

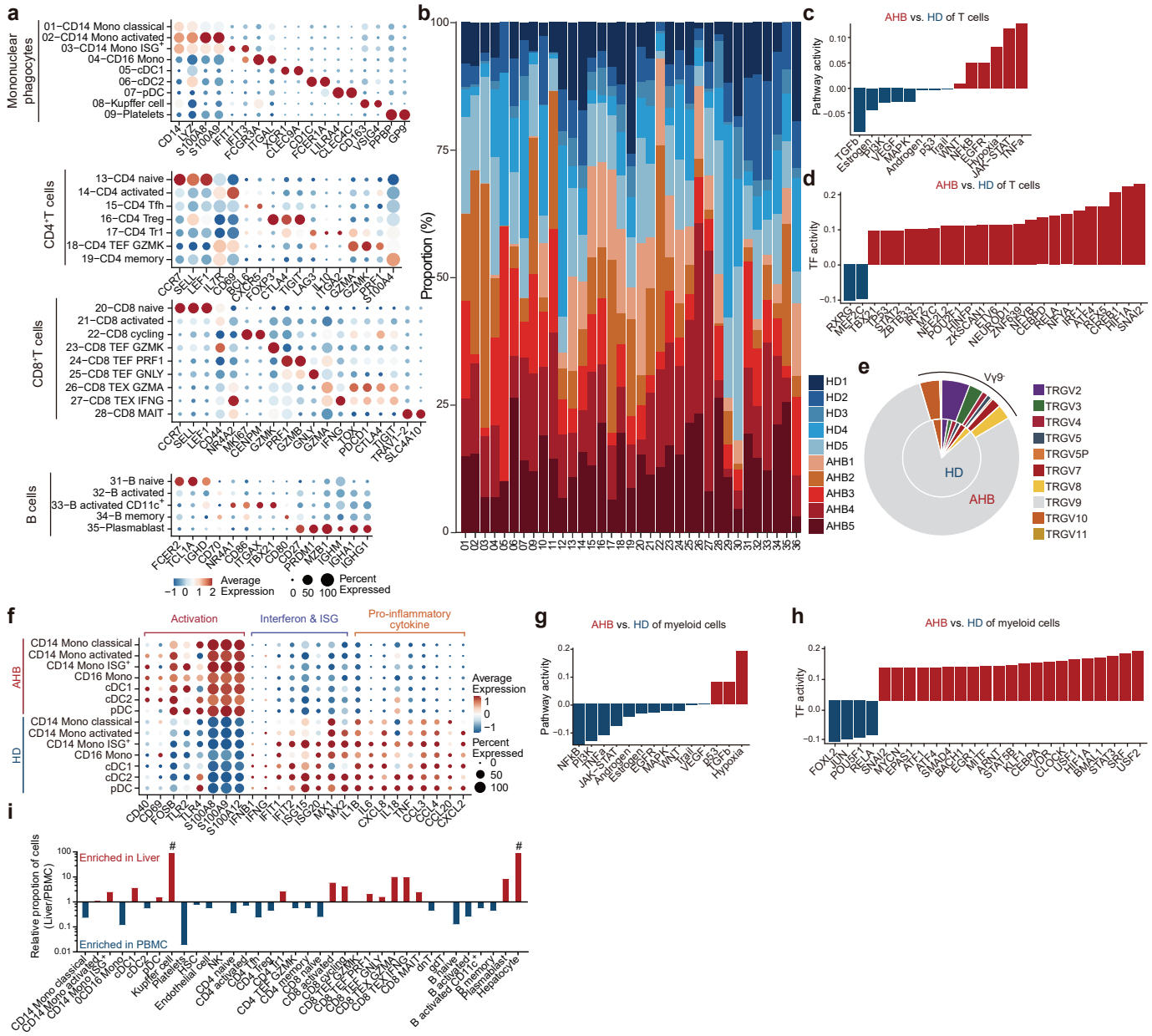
[1] Key Laboratory of Medical Molecular Virology (MOE/NHC/CAMS), Shanghai Institute of Infectious Disease and Biosecurity, Shanghai Frontiers Science Center of Pathogenic Microorganisms and Infection, School of Basic Medical Sciences, Shanghai Medical College, Fudan University, Shanghai, China

[2] Department of Infectious Diseases, Huashan Hospital, Fudan University, Shanghai, China

[†] These authors contributed equally to this work

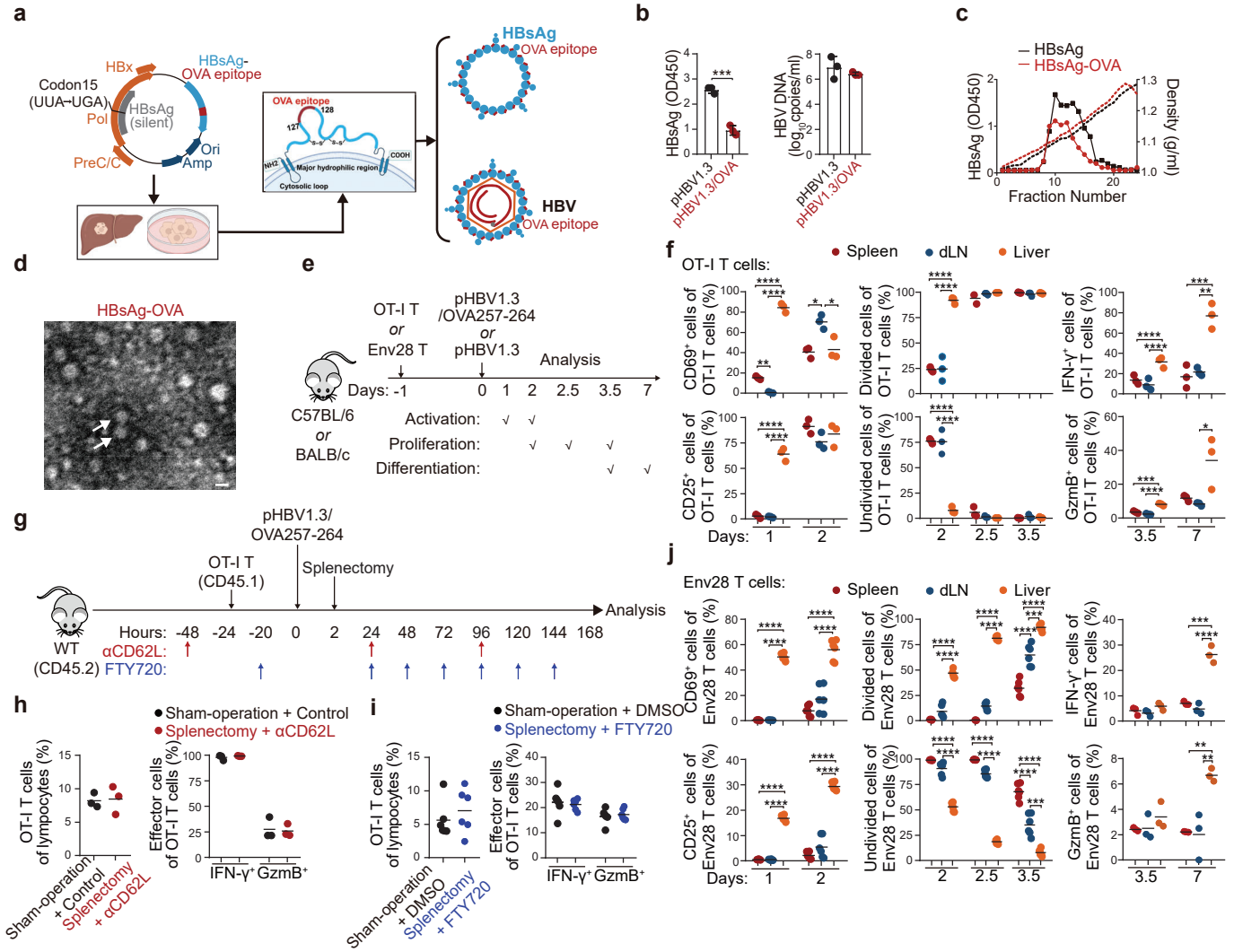
* Correspondence: zhyuan@shmu.edu.cn (Z.Y.), jianhuali@fudan.edu.cn (J. Li)

Supplementary Figure 1



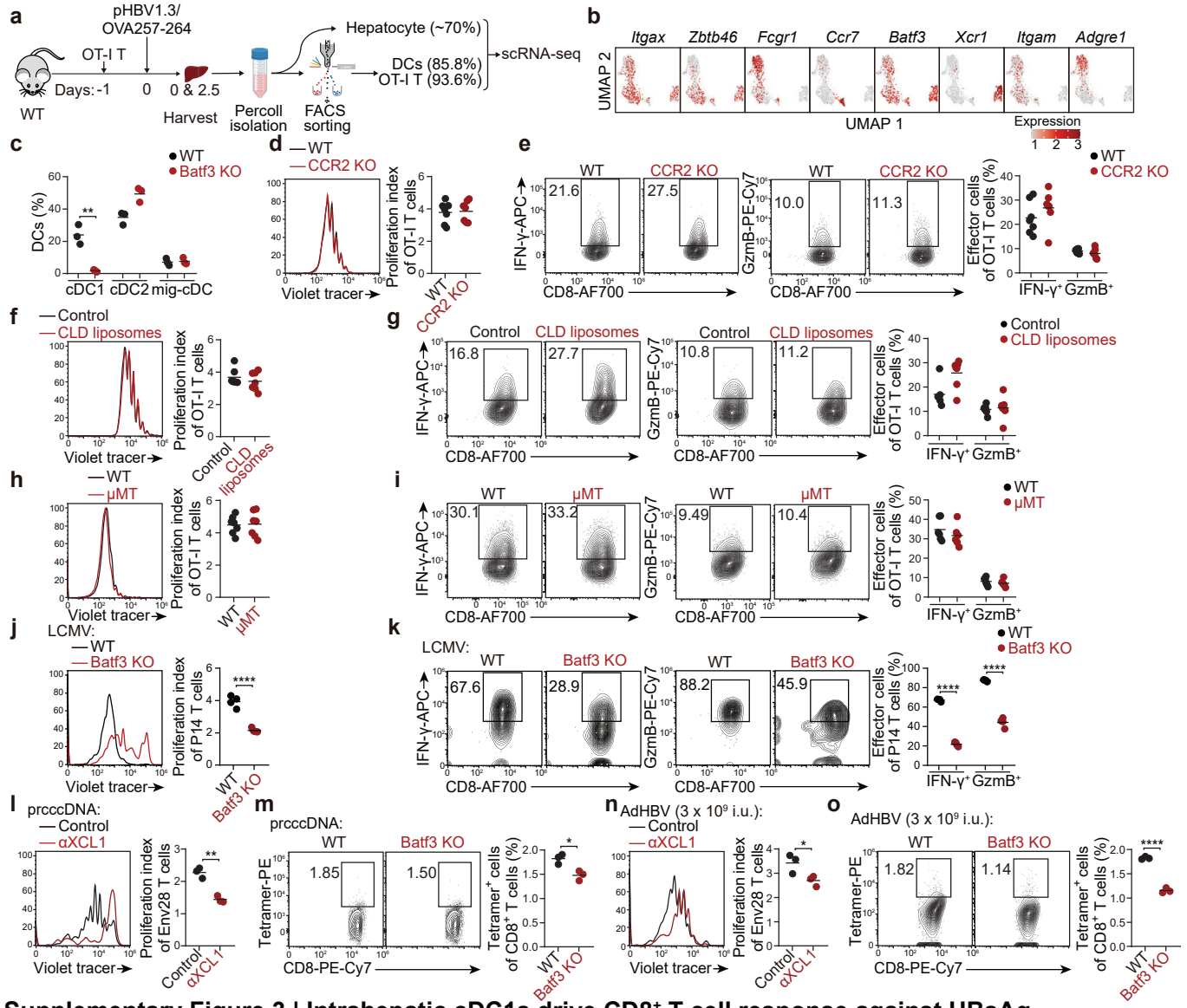
Supplementary Figure 1 | Single-cell landscape of T-cell responses in acute HBV patients.
a Dot plots representing key immune cell lineage markers. **b** Contribution of individual patients to each cell cluster across all HD and AHB samples. Each color represents a specific sample group (HD1-5 and AHB1-5). **c, d** Bar plots illustrating the activities of highly variable pathways (**c**) and transcription factors (**d**) in T cells for AHB patients versus HDs. **e** Distribution of T cell receptor gamma variable (TRGV) gene usage among γδ T cells, highlighting the presence of Vγ9⁺ T cells. The different colors represent various TRGV gene segments. **f** Dot plot displaying the expression of representative genes within the pathways highlighted in **Fig. 1h** across myeloid clusters for both AHB patients and HDs. **g, h** Bar plots illustrating the activities of highly variable pathways (**g**) and transcription factors (**h**) in myeloid cells for AHB patients versus HDs. **i** Box plots illustrating the fold enrichment of cell type proportions in the liver relative to PBMC for patient AHB3. Cell subsets that are exclusively detected in the liver are marked with '#'.

Supplementary Figure 2



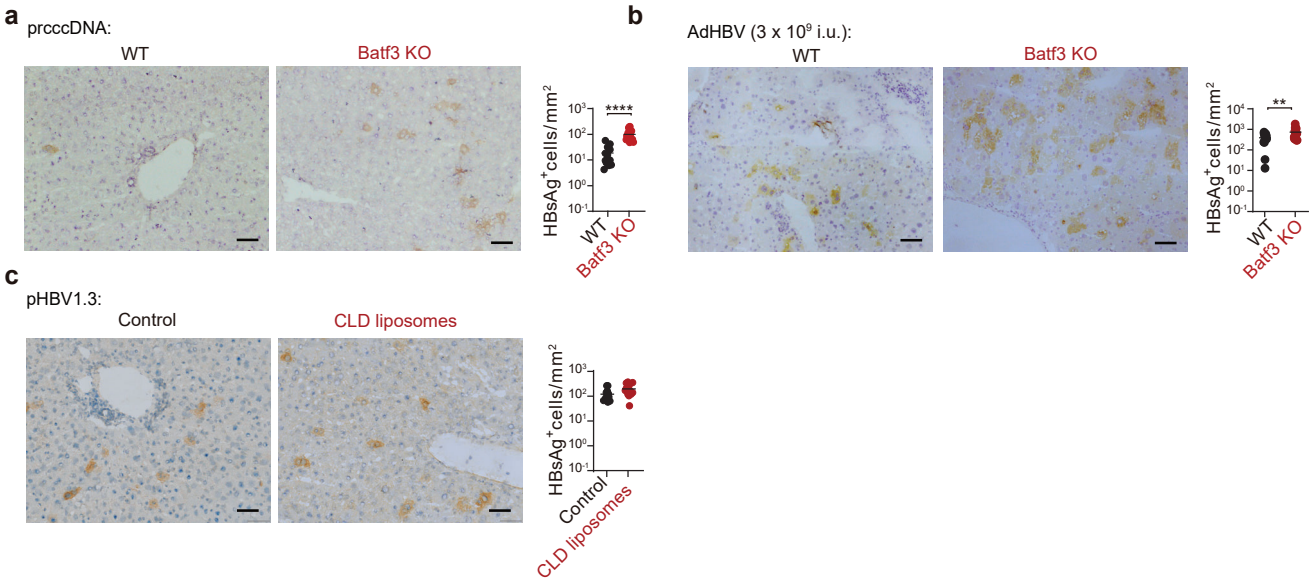
Supplementary Figure 2 | The liver is the primary site of CD8⁺ T cell priming against HBsAg in mice. **a** Diagram of pHBV1.3/OVA plasmid construct (Created with BioRender.com). **b-d** Analysis of secretion (**b**, *n* = 3 biological independent replicates), buoyant density (**c**), and particle size (arrows) (**d**) of recombinant HBsAg with OVA epitope by ELISA, sucrose-gradient ultracentrifugation, and electron microscopy, respectively. Scale bar in (**d**), 20 nm. **e** Diagram of the experimental schematic detailing the time course study of the CD8⁺ T cell response to HBsAg. **f** Percentages of CD69⁺ or CD25⁺ activated cells, divided or undivided cells, and IFN-γ⁺ or GzmB⁺ differentiated cells among OT-I T cells in the specified tissues from WT recipients at given time points post-pHBV1.3/OVA257-264 HDI (*n* = 3). **g** Diagram of the experimental schematic for (**h, i**). **h** Percentages of total, IFN-γ⁺, and GzmB⁺ OT-I T cells in the livers from WT recipients pretreated with splenectomy and anti-CD62L antibody versus sham-operation and control antibodies, at day 7 post-pHBV1.3/OVA257-264 HDI (*n* = 3). **i** Percentages of total, IFN-γ⁺, and GzmB⁺ OT-I T cells in the livers from WT recipients pretreated with splenectomy and FTY720 versus sham-operation and DMSO, at day 7 post-pHBV1.3/OVA257-264 HDI (*n* = 6). **j** Percentages of CD69⁺ or CD25⁺ activated cells, divided or undivided cells, and IFN-γ⁺ or GzmB⁺ differentiated cells among Env28 T cells in the specified tissues from WT or F1 (CD45.1/2) recipients at given time points post-pHBV1.3 HDI (*n* = 6 for activation and proliferation assays; *n* = 3 for differentiation assays). At least two independent experiments were performed. Horizontal lines of (**f, h-j**) represent median values. Error bars in (**b**) show mean ± SD. Statistical significance was calculated using two-tailed Student's *t*-tests (**b, h, i**) and One-Way ANOVA with Tukey's multiple comparisons test (**f, j**). Significance levels are indicated as: **p* < 0.05, ***p* < 0.01, ****p* < 0.001, *****p* < 0.0001. Source data and exact *p*-values are available in the Source Data file.

Supplementary Figure 3



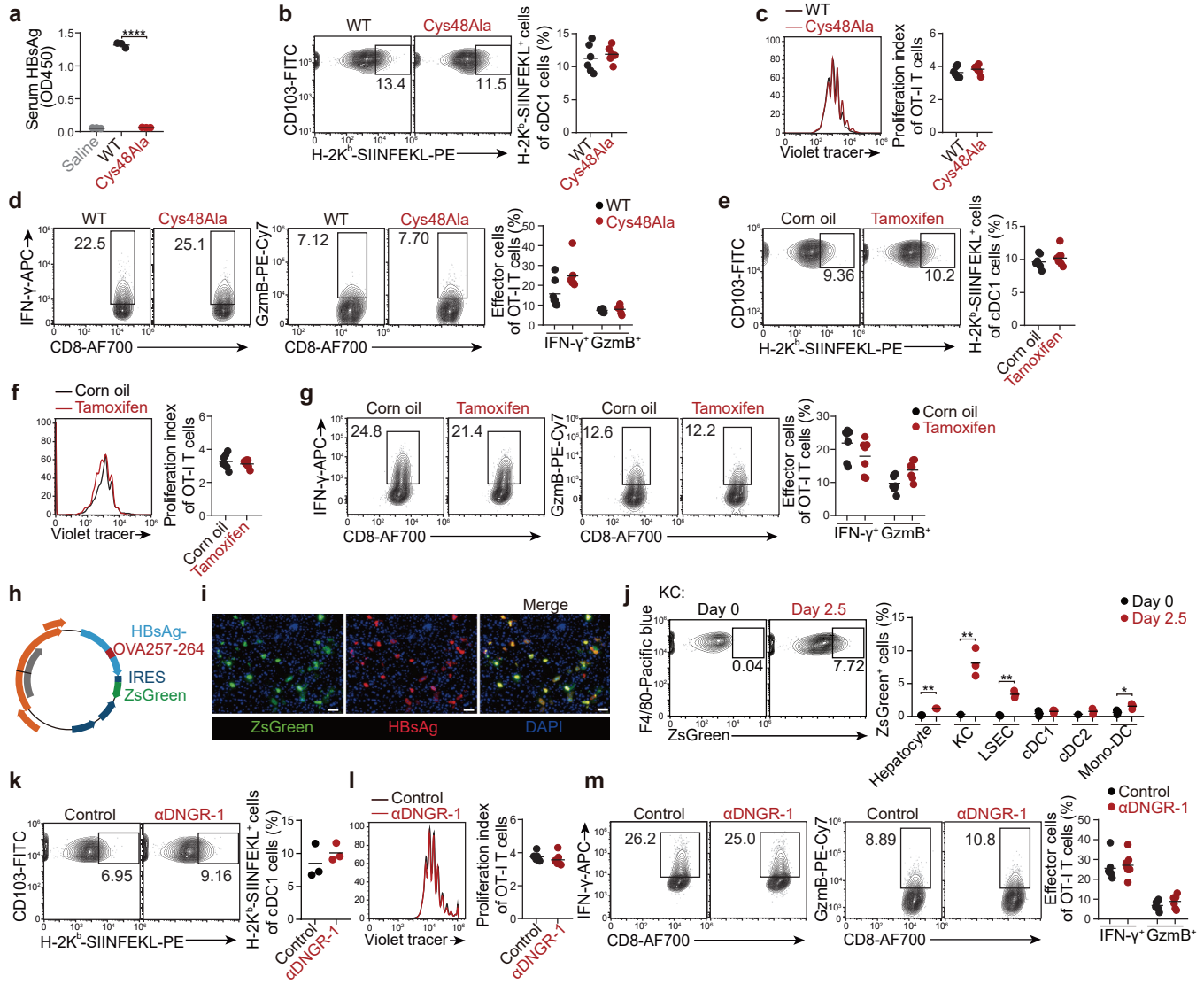
Supplementary Figure 3 | Intrahepatic cDC1s drive CD8⁺ T cell response against HBsAg. **a** Schematic illustrating the preparation of liver cells for scRNA-seq, with the cell purity and mix ratio indicated (Created with BioRender.com). **b** UMAP projections displaying the expression intensity of selected canonical cell markers. **c** Percentages of the indicated cDC subsets in the livers from Batf3 KO versus WT mice (n = 3). **d-i** Same as **Fig. 2e, f**, but in CCR2 KO mice (**d** and **e**, n = 7), WT mice treated with CLD liposomes (**f** and **g**, n = 7), or μMT mice (**h** and **i**, n = 7), compared to their respective controls. **j, k** Violet tracer-labeled P14 T cells were transferred into Batf3 KO versus WT mice, followed by LCMV Armstrong infection for 3 days. **j** Representative Violet tracer dilution and proliferation index (n = 4). **k** Representative FACS plots and percentages of IFN-γ⁺ or GzmB⁺ P14 T cells (n = 4). **l** Representative Violet tracer dilution and proliferation index of Env28 T cells in the livers from WT recipients treated with anti-XCL1 versus control antibody at day 3.5 post co-HDI with 4 μg of pCMV-Cre and 8 μg of prcccDNA (n = 3). **m** Representative FACS plots and percentages of HBV ENV353 tetramer-specific CD8⁺ T cells in the livers from Batf3 KO versus WT mice at day 5 post co-HDI with 4 μg of pCMV-Cre and 8 μg of prcccDNA (n = 3). **n** Same as (**l**), but mice were infected with 3 × 10^9 infectious units (i.u.) AdHBV (n = 3). **o** Same as (**m**), but mice were infected with 3 × 10^9 i.u. AdHBV (n = 3). At least two independent experiments were performed. The horizontal lines represent median values. Statistical significance was calculated using two-tailed Student's t-tests. Significance levels are indicated as: *p < 0.05, **p < 0.01, ***p < 0.001, ****p < 0.0001. Source data and exact p-values are available in the Source Data file.

Supplementary Figure 4



Supplementary Figure 4 | Role of myeloid cells in the clearance of intrahepatic HBsAg.
a Intrahepatic HBsAg levels in WT and Batf3 KO mice at day 14 after co-HDI with 4 μg of pCMV-Cre and 8 μg of prcccDNA (*n* = 15 view fields from 5 mice). **b** Intrahepatic HBsAg levels in WT and Batf3 KO mice at day 14 after 3 × 10^9 i.u. AdHBV infection (*n* = 15 view fields from 5 mice). **c** Intrahepatic HBsAg levels in control or CLD Liposomes treated WT mice at day 14 after pHBV1.3 HDI (*n* = 15 view fields from 5 mice). Scale bars, 50 μm. At least two independent experiments were performed. The horizontal lines represent median values. Statistical significance was calculated using two-tailed Student's *t*-tests. Significance levels are indicated as: $^{**}p < 0.01$, $^{****}p < 0.0001$. Source data and exact *p*-values are available in the Source Data file.

Supplementary Figure 5

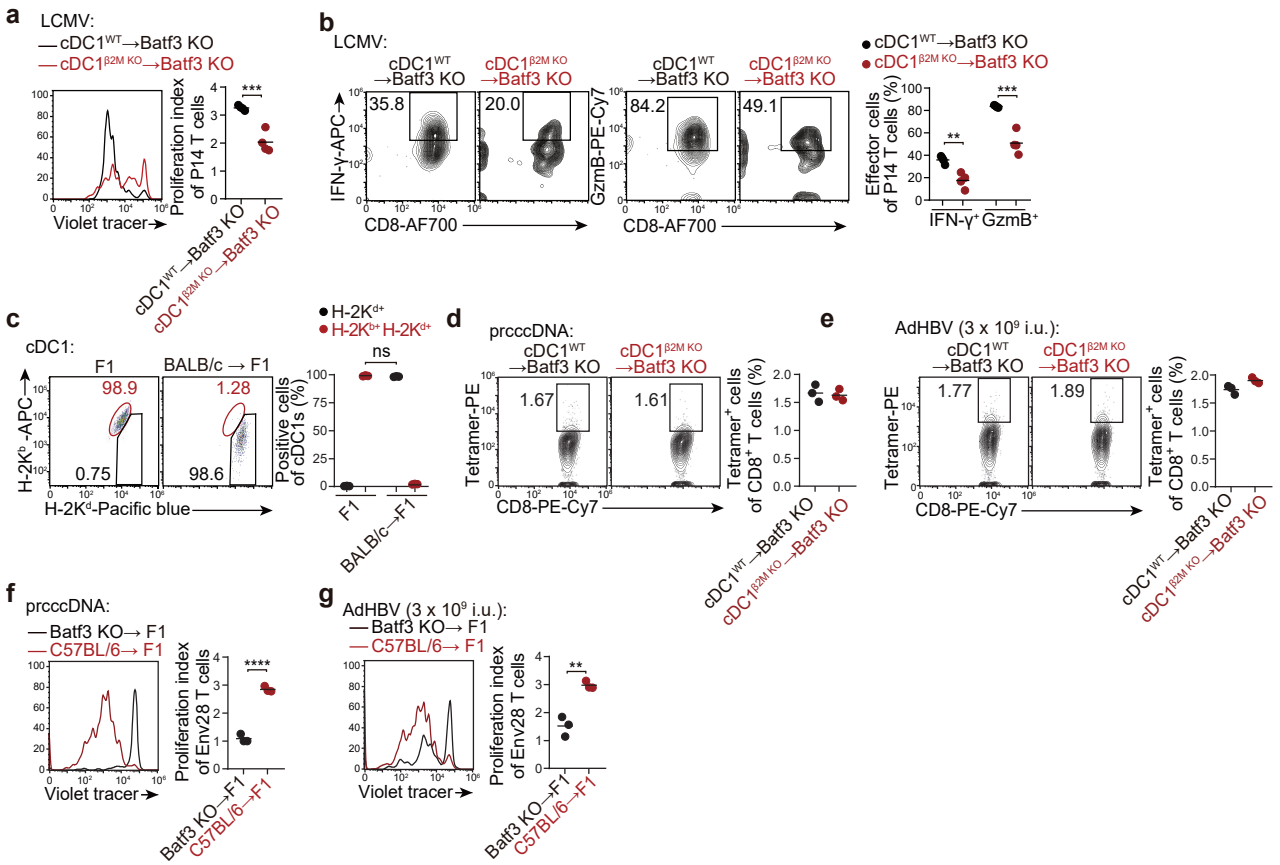


Supplementary Figure 5 | The cDC1s acquire and present HBsAg independently of cross-presentation.

a HBsAg secretion in the sera from WT mice at day 2 post-pHBV1.3/OVA257-264 (labeled "WT") or pHBV1.3/OVA257-264/Cys48Ala (labeled "Cys48Ala") HDI. **b** Representative FACS plots and percentages of H-2K^b-SIINFEKL-expressing cDC1s from WT mice at day 2.5 post-pHBV1.3/OVA257-264 or pHBV1.3/OVA257-264/Cys48Ala HDI (n = 6). **c, d** Violet tracer labeled OT-I T cells were transferred into WT mice and received pHBV1.3/OVA257-264 or pHBV1.3/OVA257-264/Cys48Ala HDI for 3.5 days. **c** Representative Violet tracer dilution and proliferation index (n = 7). **d** Representative FACS plots and percentages of IFN-γ$^+$ or GzmB$^+$ OT-I T cells (n = 7). **e** Percentages of H-2K^b-SIINFEKL-expressing cDC1s in Rab27a$^{fl/fl}$Rosa26CreERT2 mice pretreated with tamoxifen or corn oil at day 2.5 post-pHBV1.3/OVA257-264 HDI (n = 8). **f, g** Violet tracer labeled OT-I T cells were transferred into Rab27a$^{fl/fl}$Rosa26CreERT2 recipients pretreated with tamoxifen or corn oil, followed by pHBV1.3/OVA257-264 HDI for 3.5 days. **f** Representative Violet tracer dilution and proliferation index (n = 7). **g** Representative FACS plots and percentages of IFN-γ$^+$ or GzmB$^+$ OT-I T cells (n = 7). **h** Map of pHBV1.3/OVA257-264-IRES-ZsGreen construct. **i** Immunofluorescence of ZsGreen and HBsAg in the livers at day 2.5 post-pHBV1.3/OVA257-264-IRES-ZsGreen HDI. Scale bars: 50 μm. **j** Representative FACS

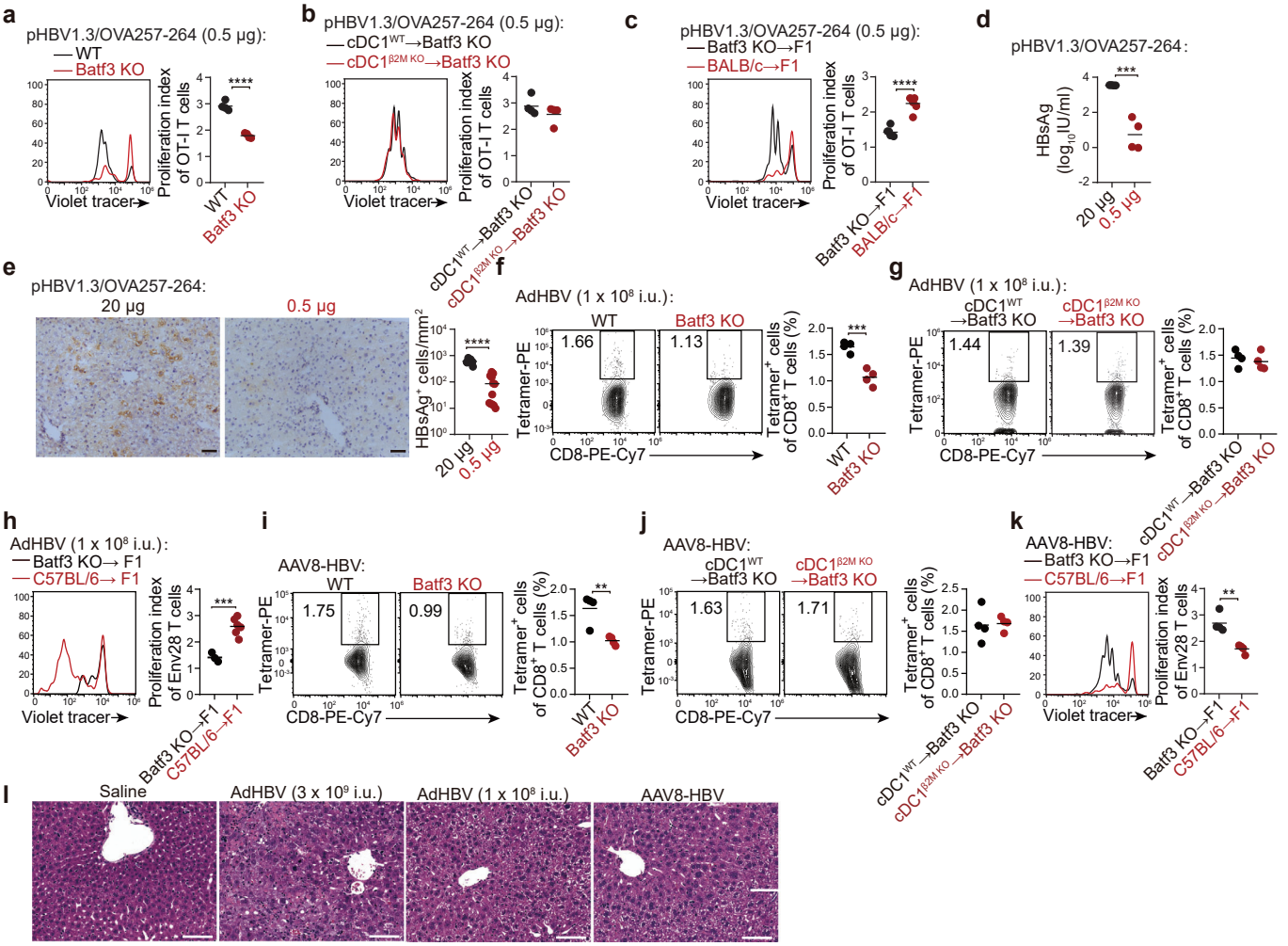
plots and percentages of ZsGreen-expressing APCs in the livers from WT mice at day 2.5 post-pHBV1.3/OVA257-264-IRES-ZsGreen HDI (*n* = 3). **k** Representative FACS plots and percentages of H-2K^{b}-SIINFEKL-expressing cDC1s from WT mice pretreated with anti-DNGR-1 versus control antibody at day 2.5 post-pHBV1.3/OVA257-264 HDI (*n* = 3). **l, m** Violet tracer-labeled OT-I T cells were transferred into WT recipients pretreated with anti-DNGR-1 versus control antibody, followed by pHBV1.3/OVA257-264 HDI for 3.5 days. **l** Representative Violet tracer dilution and proliferation index (*n* = 7). **m** Representative FACS plots and percentages of IFN-γ^{+} or GzmB^{+} OT-I T cells (*n* = 7). At least two independent experiments were performed. The horizontal lines represent median values. Statistical significance was calculated using One-way ANOVA Tukey's multiple comparisons test (**a**) and two-tailed Student's *t*-tests (**b-g, j-m**). Significance levels are indicated as: *p < 0.05, **p < 0.01 and ****p < 0.0001. Source data and exact p-values are available in the Source Data file.

Supplementary Figure 6



Supplementary Figure 6 | The cDC1s acquire and present HBsAg by MHC-I cross-dressing. **a, b** Violet tracer-labeled P14 T cells were transferred into Batf3 KO mice that were reconstituted with β2M KO versus WT cDC1s, followed by LCMV Armstrong infection for 3 days. **a** Representative Violet tracer dilution and proliferation index of P14 T cells in the livers (n = 4). **b** Representative FACS plots and percentages of IFN-γ$^+$ or GzmB$^+$ P14 T cells in the livers (n = 4). **c** Representative FACS plots and percentages of F1-or BALB/c-derived cDC1s in the livers from unirradiated F1 recipients (as a control) or F1 chimeras reconstituted with BALB/c bone marrow prior to pHBV1.3/OVA257-264 HDI (n = 3). **d** Representative FACS plots and percentages of ENV353 tetramer-specific CD8$^+$ T cells in the livers from Batf3 KO mice reconstituted with β2M KO versus WT cDC1s, at day 5 post co-HDI with 4 μg of pCMV-Cre and 8 μg of prcccDNA (n = 3). **e** Same as (**d**), but mice were infected with 3 × 10^9 i.u. AdHBV (n = 3). **f** Representative FACS plots and proliferation index of Env28 T cells in the livers from F1 chimeras reconstituted with C57BL/6 versus Batf3 KO bone marrow, at day 3.5 post co-HDI with 4 μg of pCMV-Cre and 8 μg of prcccDNA (n = 3). **g** Same as (**f**), but mice were infected with 3 × 10^9 i.u. AdHBV (n = 3). At least two independent experiments were performed. The horizontal lines represent median values. Statistical significance was calculated using two-tailed Student's t-test. Signifiance levels are indicated as: $^{**}p < 0.01$ and $^{***}p < 0.001$, *ns* = not significant. Source data and the exact p-values are available in the source Data file.

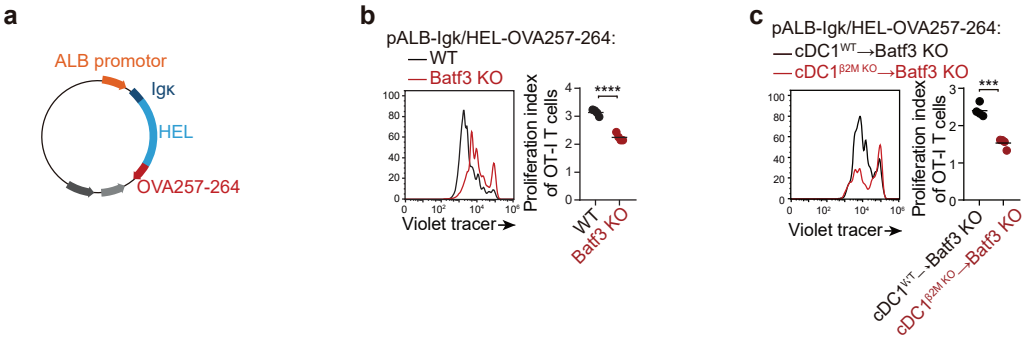
Supplementary Figure 7



Supplementary Figure 7 | cDC1 cross-dressing occurs under low antigen expression or mild inflammation.

a Representative Violet tracer dilution and proliferation index of OT-I T cells from the livers of Batf3 KO versus WT mice, at day 3.5 after 0.5 µg pHBV1.3/OVA257-264 HDI (n = 4). **b** Representative Violet tracer dilution and proliferation index of OT-I T cells from the livers of Batf3 KO mice reconstituted with β2M KO versus WT cDC1s, at day 3.5 after 0.5 µg pHBV1.3/OVA257-264 HDI (n = 4). **c** Representative Violet tracer dilution and proliferation index of OT-I T cells at day 3.5 in the livers from BALB/c versus Batf3 KO bone marrow-reconstituted F1 chimeras after 0.5 µg pHBV1.3/OVA257-264 HDI (n = 4). **d, e** Serum (**d**, n = 4) and intrahepatic (**e**, n = 15 view fields from 5 mice) HBsAg levels in WT mice at day 3 after 20 µg or 0.5 µg pHBV1.3/OVA257-264 HDI. Scale bars, 50 µm. **f** Representative FACS plots and percentages of ENV353 tetramer-specific $CD8^+$ T cells in the livers of WT and Batf3 KO mice at day 5 after AdHBV infection with a dose of 1×10^8 i.u. (n = 4). **g** Same as (**Supplementary fig. 6d**), but mice were infected with 1×10^8 i.u. AdHBV (n = 4). **h** Same as (**Supplementary fig. 6f**), but mice were infected with 1×10^8 i.u. AdHBV (n = 6). **i** Same as (**f**), but mice were infected with AAV8-HBV (n = 4). **j** Same as (**g**), but mice were infected with AAV8-HBV (n = 4). **k** Same as (**h**), but mice were infected with AAV8-HBV (n = 4). **l** Hematoxylin and eosin (H&E) -stained liver sections from the mice that were infected with AAV8-HBV or different doses of AdHBV for 3 days. Scale bars, 50 µm. At least two independent experiments were performed. The horizontal lines represent median values. Statistical significance was calculated using two-tailed Student's t-tests. Significance levels are indicated as: $^{**}p < 0.01$, $^{***}p < 0.001$, $^{****}p < 0.0001$. Source data and exact p-values are available in the Source Dat a file.

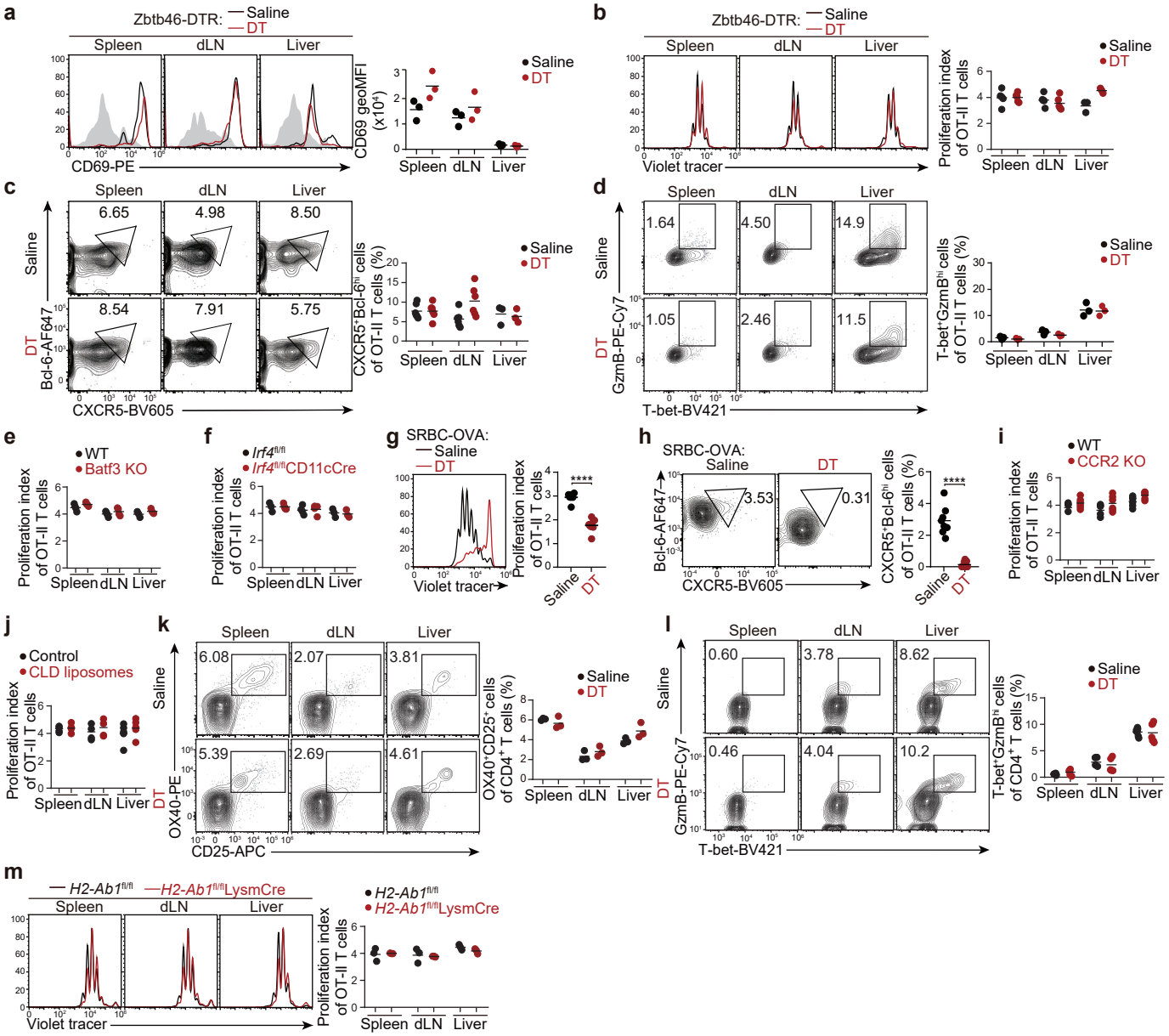
Supplementary Figure 8



Supplementary Figure 8 | cDC1 mediates HEL antigen presentation through MHC-I cross-presentation.

a Map of pALB-Igk/HEL-OVA257-264 construct. **b** Representative Violet tracer dilution and proliferation index of OT-I T cells in the Batf3 KO versus WT mice, at day 3.5 post- pALB-Igk/HEL-OVA257-264 HDI (n = 4). **c** Representative Violet tracer dilution and proliferation index of OT-I T cells in the Batf3 KO mice that were reconstituted with β2M KO versus WT cDC1s, at day 3.5 post-pALB-Igk/HEL-OVA257-264 HDI (n = 4). Three independent experiments were performed. The horizontal lines represent median values. Statistical significance was calculated using two-tailed Student's t-tests. Significance levels are indicated as: ***p < 0.001 and ****p < 0.0001. Source data and exact p-values are available in the Source Data file.

Supplementary Figure 9

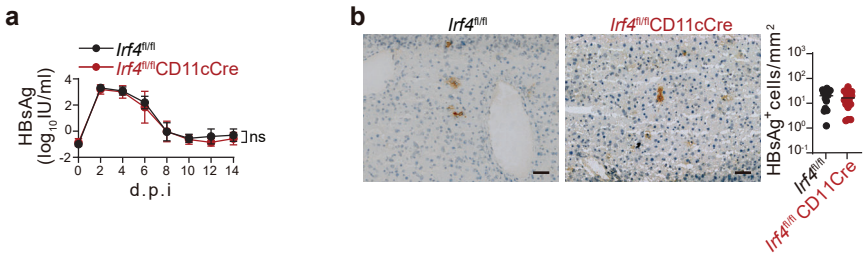


Supplementary Figure 9 | cDCs and other myeloid cells do not initiate CD4⁺ T cell responses to HBsAg.

a-d OT-II T cells, labeled with Violet tracer when needed, were transferred into Zbtb46-DTR chimeras pretreated with DT or saline, followed by pHBV1.3/OVA323-339 HDI. Spleens, dLNs, and livers were harvested from days 2 to 4.5 post-HDI. **a** Representative histogram and geoMFI data of CD69 expression at day 2 (*n* = 3). **b** Representative Violet tracer dilution and proliferation index at day 3.5 (*n* = 5 for spleen and dLN; *n* = 3 for liver). **c** Representative FACS plots and percentages of CXCR5⁺Bcl6^{hi} OT-II T cells at day 3.5 (*n* = 6 for spleen and dLN; *n* = 3 for liver). **d** Representative FACS plots and percentages of T-bet⁺GzmB^{hi} OT-II T cells at day 4.5 (*n* = 3). **e, f** Proliferation index of OT-II T cells in Batf3 KO (**e**, *n* = 3) and *Irf4*$^{fl/fl}$CD11cCre (**f**, *n* = 3) mice, compared to their respective controls at day 3.5 post-pHBV1.3/OVA323-339 HDI. **g** Same as (**b**), but mice were immunized with SRBC-OVA for 3 days, and spleens were harvested for proliferation index analysis (*n* = 7 for saline and 8 for DT treatment). **h** Same as (**c**), but mice were immunized with SRBC-OVA for 3 days, and spleens were harvested for analysis (*n* = 8).

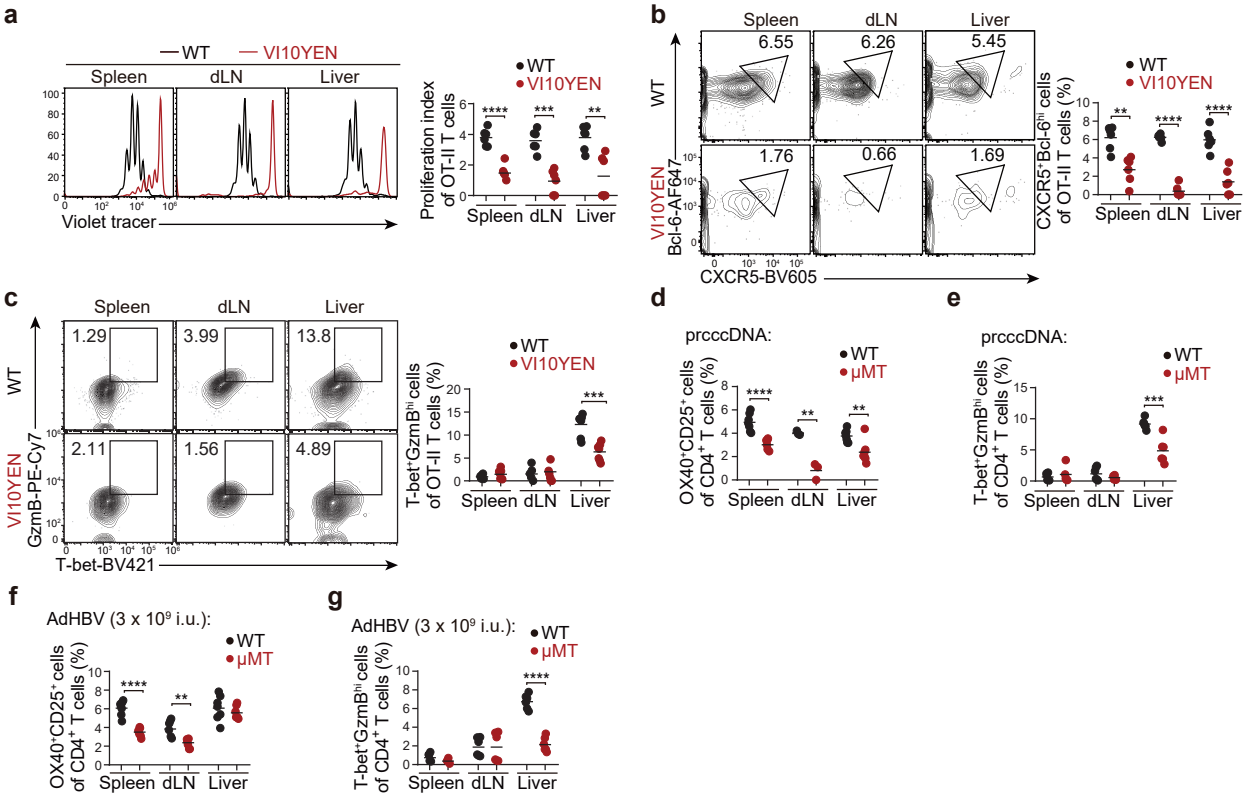
i, j Proliferation index of OT-II T cells from CCR2 KO (**i**, *n* = 6) and CLD liposomes treated (**j,** *n* = 5) WT mice, compared to their respective controls, at day 3.5 post-pHBV1.3/OVA323-339 HDI. **k, l** Representative FACS plots and percentages of endogenous $CD25^{+}OX40^{+}$ (**k**, *n* = 3) and $T\text{-}bet^{+}GzmB^{hi}$ (**l**, *n* = 7) $CD4^{+}$ T cells from Zbtb46-DTR chimeras pretreated with DT versus saline, at day 5 post-pHBV1.3 HDI. **m** Representative Violet tracer dilution and proliferation index of OT-II T cells from *H2-Ab1*$^{fl/fl}$ or *H2-Ab1*$^{fl/fl}$Lysm-Cre recipients at day 3.5 post-pHBV1.3/OVA323-339 HDI (*n* = 3). At least two independent experiments were performed. The horizontal lines represent median values. Statistical analysis were performed using two-tailed Student's *t*-tests. Significance levels are indicated as: ****$p < 0.0001$. Source data and exact *p*-values are provided in the Source Data file.

Supplementary Figure 10



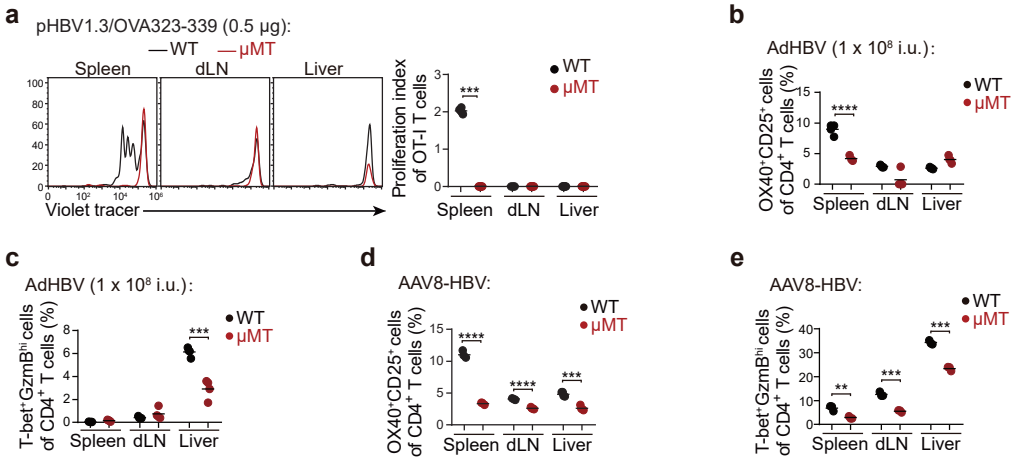
Supplementary Figure 10 | Impact of cDC2s deficiency on HBsAg clearance.
a, b Circulating (**a**, *n* = 4) and intrahepatic (**b**, *n* = 15 view fields from 4 mice) HBsAg levels in WT and *Irf4*$^{fl/fl}$CD11cCre mice post-pHBV1.3 HDI. Serum samples were collected at the indicated time points, and livers were harvested at day 14 after pHBV1.3 HDI. Scale bars, 50 μm. Three independent experiments were performed. Horizontal lines represent median values. Statistical analysis for (**a**) was conducted using two-way ANOVA, and two-tailed Student's *t*-tests for (**b**). Error bars in (**a**) show mean ± SD. Significance levels are indicated as: *ns* = not significant. Source data and exact *p*-values are provided in the Source Data file.

Supplementary Figure 11



Supplementary Figure 11 | B cells initiate CD4⁺ T cell responses to HBsAg.
a-c OT-II T cells, labeled with Violet tracer when needed, were transferred into VI10YEN versus WT mice, followed by pHBV1.3/OVA323-339 HDI. Spleens, dLNs, and livers were harvested for FACS analysis from days 3.5 to 4.5 post-HDI. **a** Representative Violet tracer dilution and proliferation index at day 3.5 (n = 6). **b** Representative FACS plots and percentages of CXCR5⁺Bcl6^{hi} OT-II T cells at day 3.5 (n = 6). **c** Representative FACS plots and percentages of T-bet⁺GzmB^{hi} OT-II T cells at day 4.5 (n = 7). **d, e** Percentages of endogenous CD25⁺OX40⁺ (**d**, n = 7 for spleen and liver; n = 3 for dLN) and T-bet⁺GzmB^{hi} (**e**, n = 6) CD4⁺ T cells in the spleens, dLNs, and livers from µMT versus WT recipients, at day 5 post co-HDI with 4 µg of pCMV-Cre and 8 µg of prcccDNA. **f, g** Same as (**d, e**), but mice were infected with 3 × 10⁹ i.u. AdHBV (**f**, n = 7; **g**, n = 6). At least two independent experiments were performed. The horizontal lines represent median values. Statistical analysis were performed using two-tailed Student's t-tests. Significance levels are indicated as: $^{**}p < 0.01$, $^{***}p < 0.001$, and $^{****}p < 0.0001$. Source data and exact p-values are provided in the Source Data file.

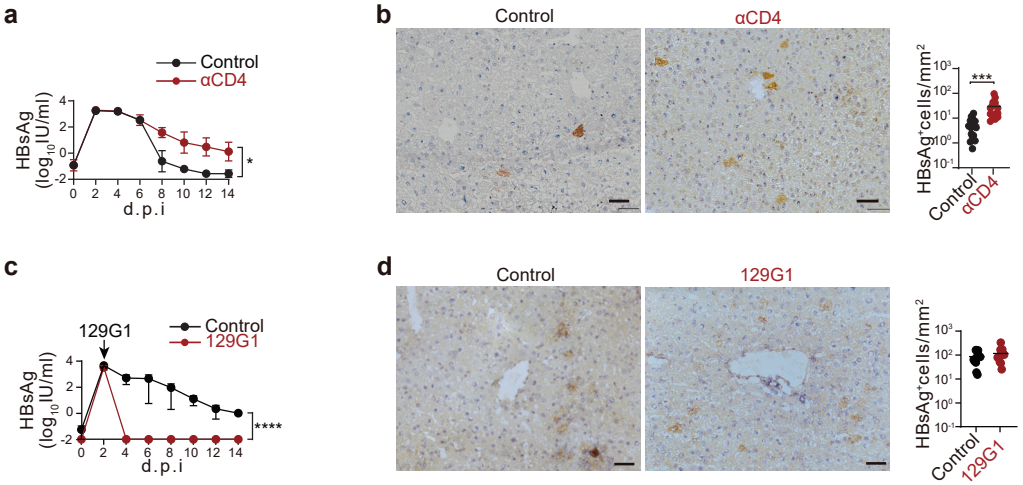
Supplementary Figure 12



Supplementary Figure 12 | B cells initiate CD4⁺ T cell responses under low antigen expression or mild inflammation.

a Representative Violet tracer dilution and proliferation index of OT-II T cells in the spleens, dLNs, and livers from µMT versus WT mice, at day 3.5 after 0.5 µg pHBV1.3/OVA323-339 HDI (n = 6). **b, c** Percentages of endogenous CD25⁺OX40⁺ (**b**, n = 7) and T-bet⁺GzmB^hi (**c**, n = 6) CD4⁺ T cells in the spleens, dLNs, and livers from µMT versus WT mice at day 5 after 1 × 10^8 i.u. AdHBV infection (n = 4). **d, e** Same as (**b, c**), but mice were infected with AAV8-HBV (n = 4). At least two independent experiments were performed. The horizontal lines represent median values. Statistical analysis were performed using two-tailed Student's t-tests. Significance levels are indicated as: **p < 0.01, ***p < 0.001, and ****p < 0.0001. Source data and exact p-values are provided in the Source Data file.

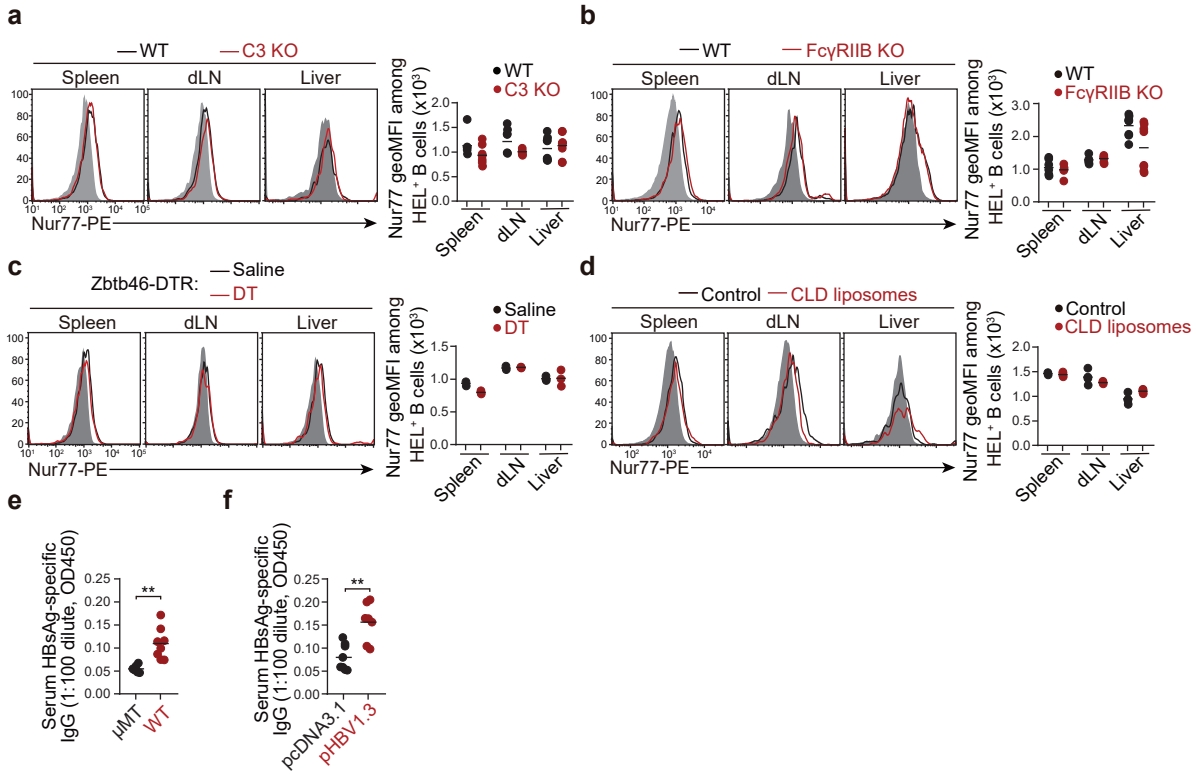
Supplementary Figure 13



Supplementary Figure 13 | Effects of CD4⁺ T cell depletion and 129G1 antibody administration on HBsAg clearance.

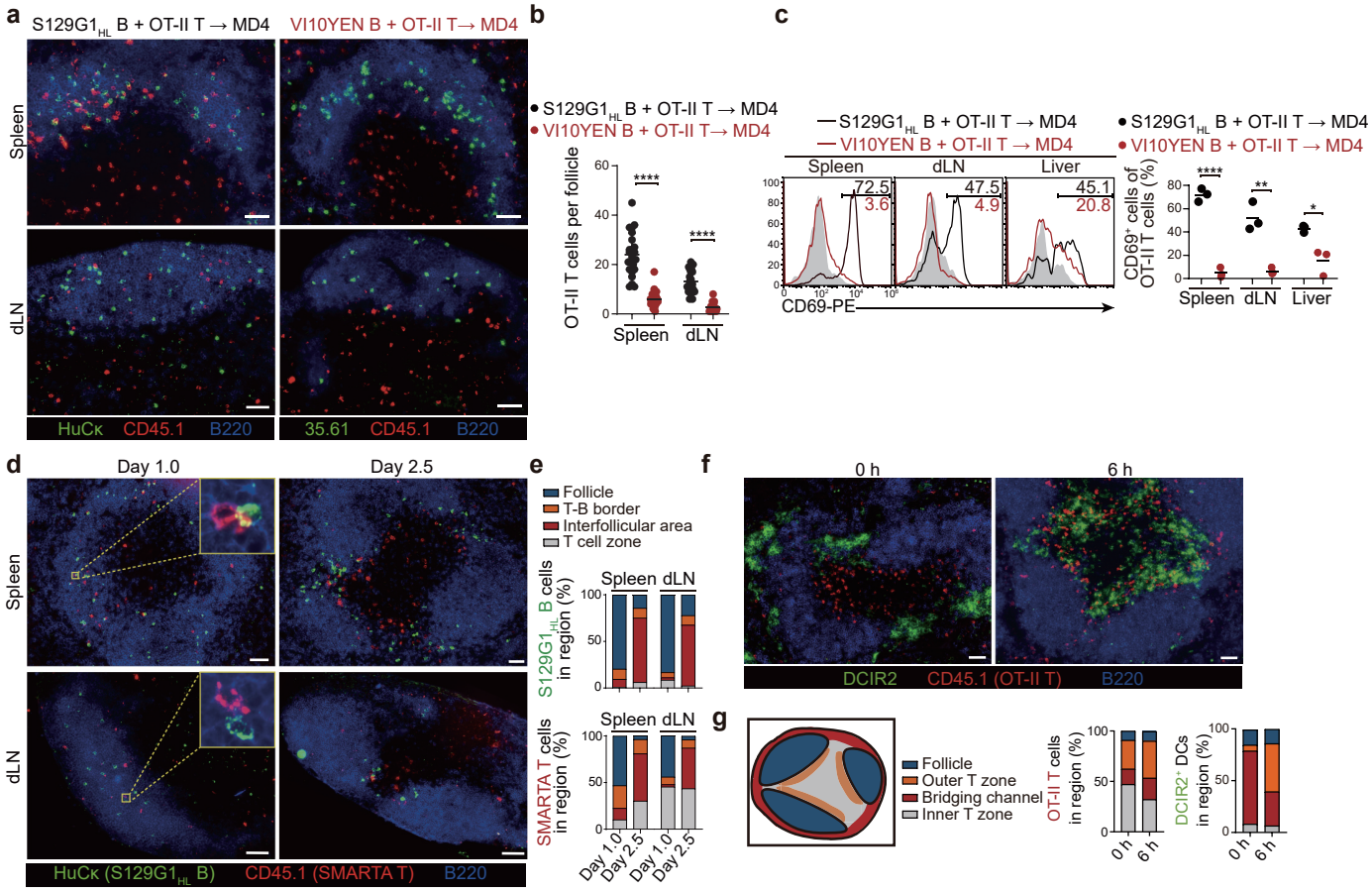
a, b Circulating (**a**, *n* = 4 mice for control antibody treated and 3 mice for anti-CD4 antibody treated) and intrahepatic (**b**, *n* = 15 view fields from 4 mice) HBsAg levels in WT mice treated with anti-CD4 or control antibody. **c, d** Circulating (**c**, *n* = 4) and intrahepatic (**d**, *n* = 15 view fields from 4 mice) HBsAg levels in μMT mice treated with control or 129G1 antibody. Serum samples were collected at the indicated time points, and liver tissues were harvested on day 14 post-pHBV1.3 HDI. Scale bars, 50 μm. At least two independent experiments were performed. Error bars in (**a, c**) show mean ± SD. Horizontal lines in (**b, d**) represent median values. Statistical analyses for (**a, c**) were conducted using two-way ANOVA, and two-tailed Student's *t*-tests for (**b, d**). Significance levels are indicated as: **p* < 0.05, ****p* < 0.001, and *****p* < 0.0001. Source data and exact *p*-values are provided in the Source Data file.

Supplementary Figure 14



Supplementary Figure 14 | Soluble HEL accesses follicular B cells independently of opsonization. **a, b** Representative histograms and geoMFI data of Nur77 expression in transferred Hy10 B cells in the spleens, dLNs, and livers of C3 KO (**a**) and FcγRIIB KO (**b**) mice, compare to their respective WT controls, at 18 hours post-pALB-Igκ/HEL HDI (n = 8). **c, d** Representative histograms and geoMFI data of Nur77 expression in transferred Hy10 B cells in the spleens, dLNs, and livers of Zbtb46-DTR chimeras treated with DT (**c**, n = 3) or CLD liposomes treated WT mice (**d**, n = 4), compared to their respective controls, at 18 hours post-pALB-Igκ/HEL HDI. **e** Serum HBsAg-specific IgG levels from WT and μMT mice (n = 7 for μMT mice; n = 7 for WT mice). **f** Serum HBsAg-specific IgG levels from mice that underwent HDI with either pcDNA3.1 or pHBV1.3 for 18 hours (n = 8 for the pcDNA3.1 group; n = 7 for the pHBV1.3 group). At least two independent experiments were performed. The horizontal lines represent median values. Statistical analysis was performed using two-tailed Student's t-tests. Significance levels are indicated as: $^{**}p < 0.01$. Source data and exact p-values are provided in the Source Data file.

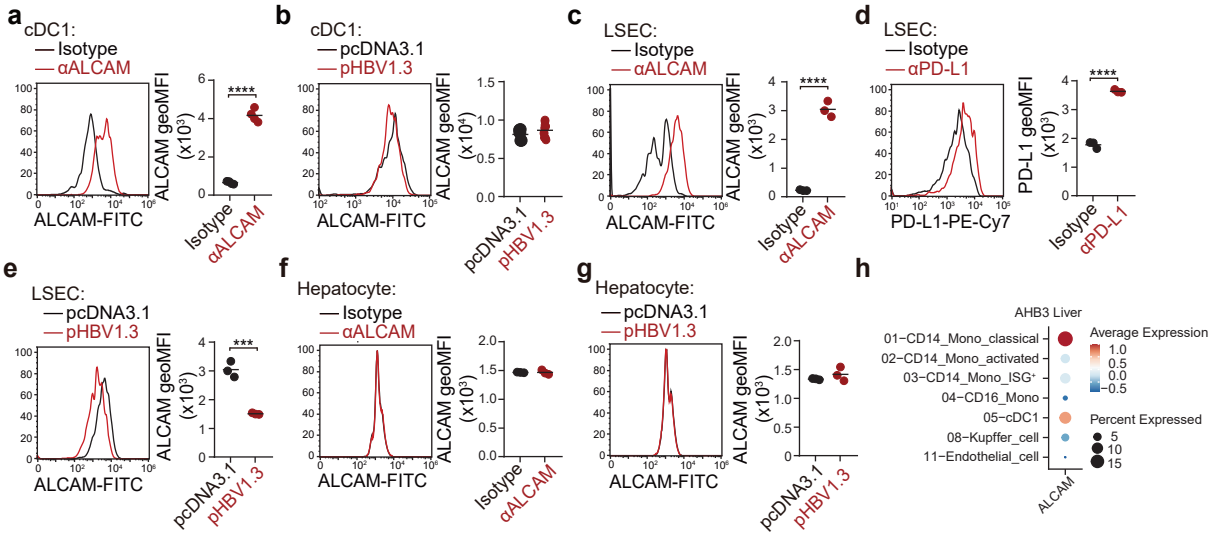
Supplementary Figure 15



Supplementary Figure 15 | B cells sequentially initiate CD4⁺ T cell responses in follicular and interfollicular regions.

a, b Immunofluorescence of co-transferred S129G1$_{HL}$ (HuCκ, green) or VI10YEN B cells (anti-idiotypic antibody 35.61, green), along with OT-II T cells (CD45.1, red) in the spleens (top) and dLNs (bottom) of MD4 mice at day 1 post-pHBV1.3/OVA323-339 HDI (**a**), with quantification of OT-II T cells within B cell follicles (**b**; *n* = 23 follicle regions from the spleen S129G1$_{HL}$ B cell group, *n* = 31 follicle regions from the spleen V10YEN B cell group, and *n* = 20 follicle regions from both dLNs groups, totaling 6 mice). **c** Representative histograms and percentages of CD69⁺ OT-II T cells in the spleens, dLNs, and livers from the mice described in (**a**, *n* = 3). **d** Immunofluorescence of S129G1$_{HL}$ B cells (HuCκ, green), SMARTA T cells (CD45.1, red), and endogenous B cells (B220, blue) in the spleens (top) and dLNs (bottom) from WT recipients at the indicated time points post-pHBV1.3/GP66-80 HDI. **e** Quantification of S129G1$_{HL}$ B cells (top) and SMARTA T cells (bottom) in the specified regions of spleens and dLNs stained in (**d**, *n* = 9 white pulp areas of the spleen from 3 mice and *n* = 9 LN slices from 3 mice). **f** Immunofluorescence of OT-II T cells (CD45.1, red), cDC2 cells (DCIR2, green), and endogenous B cells (B220, blue) in the spleens from WT recipients at the indicated time points after SRBC-OVA immunization. **g** Schematic illustration of the spatial organization of B and T cell zone and their interfaces in spleen (left), with quantification of OT-II T cells (middle) and DCIR2⁺ DCs (right) in the specified regions stained in (**f**). Scale bars in (**a, d, f**), 50 μm. Data are representative of three independent experiments. Horizontal lines of (**b, c**) represent median values. Data in (**e, f**) represent the relative proportions of each group. Statistical analysis was performed using two-tailed Student's *t*-tests. Significance levels are indicated as: **p* < 0.05, ***p* < 0.01, and *****p* < 0.0001. Source data and exact *p*-values are provided in the Source Data file.

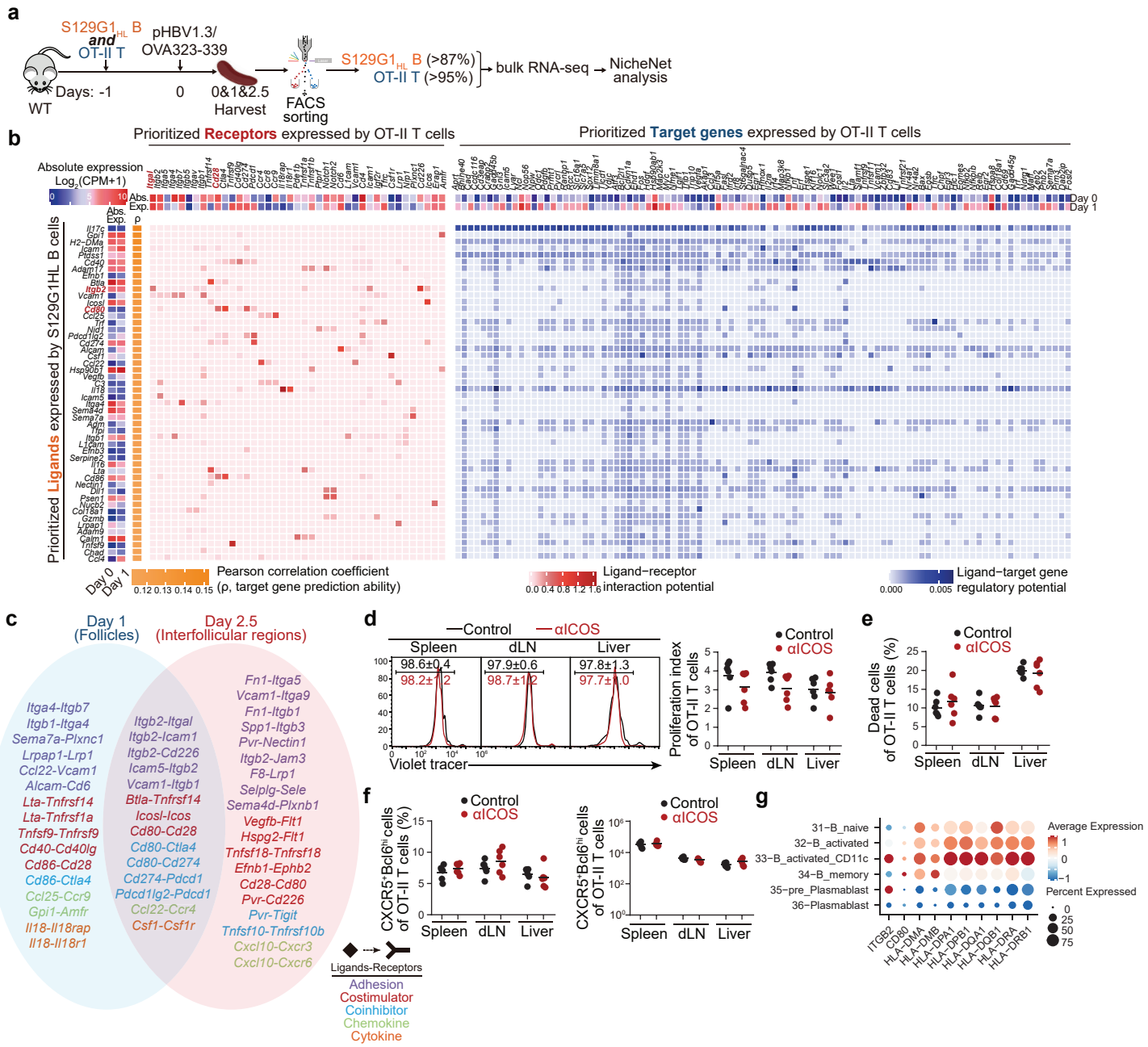
Supplementary Figure 16



Supplementary Figure 16 | ALCAM and PD-L1 expression levels in liver cells of mice and AHB patients.

a, b Representative histogram and geoMFI data of ALCAM expression on cDC1s from the livers of naïve mice compared to isotype control (**a**) and from pHBV1.3 versus pcDNA3.1 HDI mice (**b**). Measurements were taken two days post-HDI (n = 6). **c-e** Representative histogram and geoMFI data showing ALCAM (**c,** n = 3) and PD-L1 (**d**, n = 3) expression on LSECs from the livers of naïve mice compared to isotype controls, and the expression of ALCAM on LSECs from the livers of pHBV1.3 versus pcDNA3.1 HDI mice (**e**, n = 3). **f, g** Representative histogram and geoMFI data of ALCAM expression on hepatocytes from the livers of naïve mice compared to isotype control (**f**, n = 3) and from pHBV1.3 versus pcDNA3.1 HDI mice (**g,** n = 3), with measurements taken two days post-HDI. **h** Dot plot illustrating ALCAM mRNA expression in the liver cells from one AHB liver, derived from scRNA-seq data in **Fig. 1a**. At least two independent experiments were performed. The horizontal lines represent median values. Statistical analysis was performed using two-tailed Student's t-tests. Significance levels are indicated as: ***$p < 0.001$ and ****$p < 0.0001$. Source data and exact p-values are provided in the Source Data file.

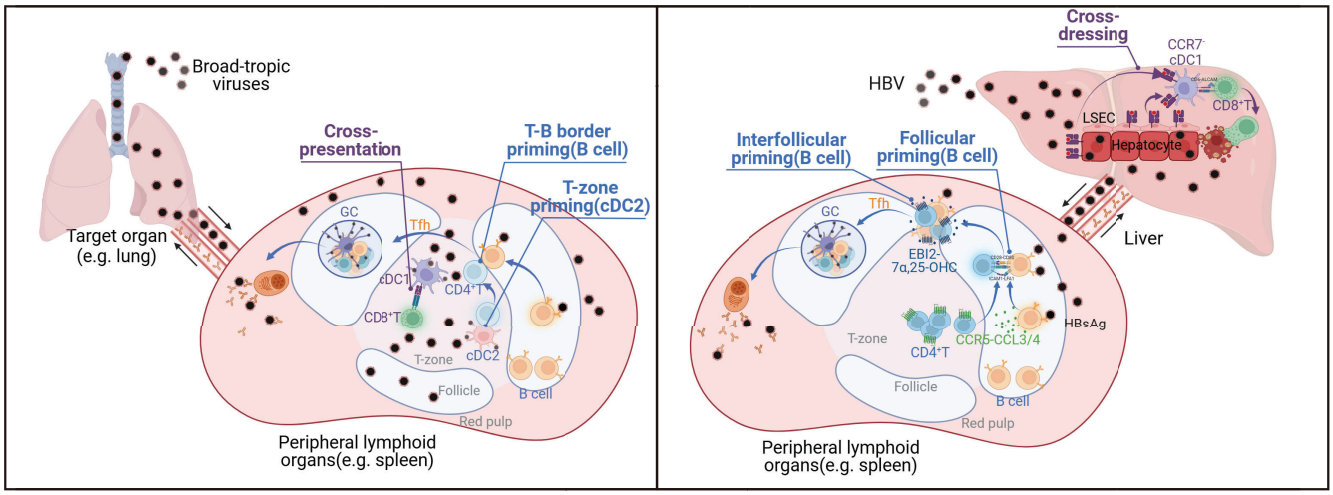
Supplementary Figure 17



Supplementary Figure 17 | Deciphering cellular crosstalk landscape associated with CD4⁺ T cell priming.

a Schematic illustrating the preparation of spleen cells for bulk RNA-seq (Created with BioRender.com). **b** Ligand activities (left, brown), potential receptors (middle, red), and predicted target genes (right, blue) identified by NicheNet analysis based on the key signature genes of transferred OT-II T cells in the spleens from WT mice, at day 1 after HDI of pHBV1.3/OVA323-339. Heatmaps for absolute expression of ligands, receptors, and target genes are also shown. **c** Venn diagram showing overlaps and differences in ligand-receptor pairs of crosstalk from $S129G1_{HL}$ B cells to OT-II T cells between day 1 and day 2.5 after HDI. **d** Representative FACS plots and proliferation index of OT-II T cells in spleens, dLNs, and livers from WT mice treated with control or anti-ICOS antibody, at day 3.5 post-HDI of pHBV1.3/OVA323-339 (n = 6). **e** Percentages of dead OT-II cells within transferred OT-II T cells in spleens, dLNs, and livers from the mice described in (**d**), using the viability dye eFluor 780 (n = 6). **f** Percentages and numbers of $CXCR5^{+}Bcl6^{hi}$ cells within transferred OT-II T cells in spleens, dLNs, and livers from the mice described in (**d**) (n = 6). **g** Dot plot illustrating *ITGB2*, *CD80*, and *HLA-II* mRNA expression in HBsAg-specific B cells from PBMCs of foure AHB patients. At least two independent experiments were performed. The horizontal lines represent median values. Source data and exact *p*-values are provided in the Source Data file.

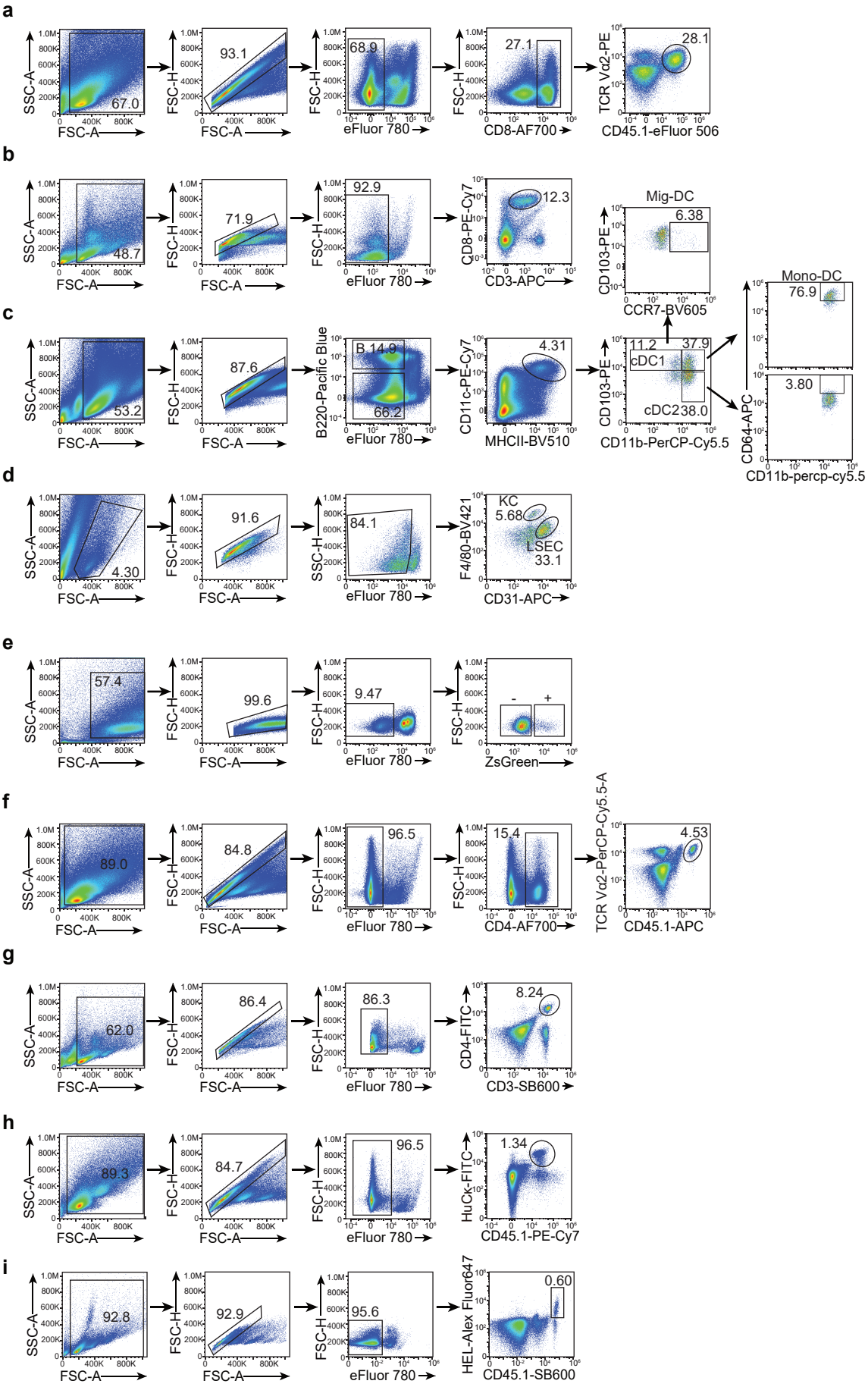
Supplementary Figure 18



Supplementary Figure 18 | Mechanistic comparison of antigen presentation.
Broad-tropic virus infection (left): Upon some broad-tropic virus infections (or some vaccine immunization), a wide range of cells spanning peripheral to lymphoid tissues become targets, leading to an influx of pattern-recognition receptor ligands and antigens apt for antigen-presenting cells. Peripheral migratory cDCs transport these antigens to dLN-resident cDCs. Moreover, dLN and spleen-resident cDCs may directly internalize viral antigens. After processing, cDC1s, through MHC-I cross-presentation, facilitate $CD8^+$ T cell differentiation. These $CD8^+$ T effector cells then work to control the viral load in both lymphoid and peripheral tissues. cDC2s present antigens to $CD4^+$ T cells via MHC-II, thus triggering their differentiation, including the early stages of Tfh cell development. Simultaneously, B cells capture viral antigens from $CD169^+$ macrophages and navigate to T-B borders, further amplifying Tfh differentiation.

HBV infection (right): Due to the unique replication pattern of HBV, which is confined to hepatocytes but results in the production and secretion of HBsAg in large quantities, the adaptive immune system encounters a distinctive challenge in acquiring HBsAg and initiating an immune response. Here, the liver, as the primary target organ for the virus, plays a pivotal role in $CD8^+$ T cell priming against HBsAg. Within the liver, $Batf3^+XCR1^+CCR7^-$ cDC1s present hepatocyte-derived HBsAg via MHC-I cross dressing, triggering the $CD8^+$ T cell response against HBsAg. Upon HBsAg access to lymphoid tissues, B cells take precedence over cDCs in initiating $CD4^+$ T cell differentiation in lymphoid tissues. They directly acquire non-opsonized HBsAg within the spleen and dLN. These B cells transition from the follicular zones to the interfollicular zones, guided by the CCL3/4-CCR5 and 7α,25-OHC-EBI2 axes, and sequentially induce HBsAg-specific $CD4^+$ T cell responses at these two zones (Created with BioRender.com).

Supplementary Figure 19



Supplementary Figure 19 | Gating strategy for flow cytometric analysis.
a Gating strategy for the flow cytometric analysis in Figures 2e-h, 3b, 3c, 3e, S2f, S2h, S2i, S3d-i, S5c, S5d, S5f, S5g, S5l, S5m, S7a-c, S8b, and S8c. **b** Gating strategy for the flow cytometric analysis in Figures 2k, 2l, 3g, S3m, S3o, S6d, S6e, S7f, S7g, S7i, and S7j. **c** Gating strategy for the flow cytometric analysis in Figures 2c, 2d, 3f, 3k, 3l, S3c, S5b, S5e, S5j, S5k, S6c, S16a, and S16b. **d** Gating strategy for the flow cytometric analysis in Figures 2c, 2d, 3l, S5j, and S16c-e. **e** Gating strategy for the flow cytometric analysis in Figures 2c, 2d, S5j, S16f, and S16g. **f** Gating strategy for the flow cytometric analysis in Figures 4a-d, 4g, 7e, 7j, 9b-g, S9a-j, S9m, S11a-c, S12a, S15c, and S17d-f. **g** Gating strategy for the flow cytometric analysis in Figures 4e, 4f, S9k, S9l, S11d-g, and S12b-e. **h** Gating strategy for the flow cytometric analysis in Figures 5d-f, 5h-k, and 7b. **i** Gating strategy for the flow cytometric analysis in Figures S14a-d.

Supplememtary Table 1. List of antibodies used in this study.

REAGENT or RESOURCE	SOURCE	IDENTIFIER
Antibodies		
Alexa Fluor 700 anti-mouse CD4, clone GK1.5, dilution 1:100	BioLegend	Cat# 100430; RRID:AB_493699
FITC anti-mouse CD4, clone RM4-5 dilution 1:100	BD Biosciences	Cat# 553047; RRID:AB_394583
PE anti-mouse CD4, clone GK1.5 dilution 1:100	BioLegend	Cat# 100408; RRID:AB_312693
Alexa Fluor 700 anti-mouse CD8α, clone 53-6.7, dilution 1:100	BioLegend	Cat# 100730; RRID:AB_493703
FITC anti-mouse CD8α, clone 53-6.7, dilution 1:100	BioLegend	Cat# 100706; RRID:AB_312745
PE/Cyanine7 anti-mouse CD8a, clone 53-6.7, dilution 1:100	BioLegend	Cat# 100722; RRID:AB_2563946
APC anti-mouse CD45.1, clone A20, dilution 1:100	BioLegend	Cat# 110714; RRID:AB_313503
FITC anti-mouse CD45.1, clone A20, dilution 1:100	eBioscience	Cat# 11-0453-85; RRID:AB_465059
PE/Cyanine7 anti-mouse CD45.1, clone A20, dilution 1:100	BioLegend	Cat# 110730; RRID:AB_1134168
Super Bright 436 anti-mouse CD45.1, clone A20, dilution 1:100	eBioscience	Cat# 62-0453-82; RRID:AB_2734990
PerCP/Cyanine5.5 anti-mouse TCR Vα 2, clone B20.1, dilution 1:100	BioLegend	Cat# 127814; RRID:AB_1186116
PE anti-mouse TCR Vα2, clone B20.1	BioLegend	Cat# 127808; RRID:AB_1134183
Biotin anti-mouse CD185 (CXCR5), clone 2G8, dilution 1:100	BD Biosciences	Cat# 551960; RRID:AB_394301
Biotin anti-mouse CD45.1, clone A20, dilution 1:200	eBioscience	Cat# 13-0453-85; RRID:AB_466454
eFluor 506 anti-mouse CD45.1, clone A20, dilution 1:100	eBioscience	Cat# 69-0453-82; RRID:AB_2637183
Biotin anti-mouse CD45.2, clone 104, dilution 1:200	eBioscience	Cat# 13-0454-85; RRID:AB_466457
PE/Cyanine7 anti-mouse CD279 (PD-1), clone RMP1-30, dilution 1:100	BioLegend	Cat# 109110; RRID:AB_572017
Brilliant Violet 421 anti- T-bet, clone 4B10, dilution 1:100	BioLegend	Cat# 644815; RRID:AB_10896427
APC anti-T-bet, clone 4B10, dilution 1:100	eBioscience	Cat# 17-5825-82; RRID:AB_2744712
Alexa Fluor 647 anti-mouse/human Bcl6, clone IG191E/A8, dilution 1:100	BioLegend	Cat# 648306; RRID:AB_2565299

Brilliant Violet 421 anti-mouse Bcl6, clone K112-91, dilution 1:100	BD Biosciences	Cat# 563363; RRID:AB_2738159
PE/Cyanine7 anti-mouse Granzyme B, clone NGZB, dilution 1:100	eBioscience	Cat# 25-8898-82; RRID:AB_10853339
FITC ant-mouse I-Ab, clone AF6-120.1, dilution 1:100	BioLegend	Cat# 116406; RRID:AB_313725
APC anti-mouse I-Ab, clone AF6-120.1, dilution 1:100	BioLegend	Cat# 116418; RRID:AB_10574160
PE/Cyanine7 anti-mouse CD11c, clone N418, dilution 1:100	BioLegend	Cat# 117318; RRID:AB_493568
Brilliant Violet 510™ anti-mouse I-A/I-E, clone M5/114.15.2, dilution 1:100	BioLegend	Cat# 107636; RRID:AB_2561397
PerCP/Cyanine5.5 anti-mouse/human CD11b, clone M1/70, dilution 1:100	BioLegend	Cat# 101228; RRID:AB_893232
FITC anti-mouse/human CD11b, clone M1/70, dilution 1:100	BioLegend	Cat# 101206; RRID:AB_312789
PE anti-mouse CD103, clone M290, dilution 1:100	BD Biosciences	Cat# 557495; RRID:AB_396732
FITC anti-mouse CD103, clone 2E7, dilution 1:100	BioLegend	Cat# 121420; RRID:AB_10714791
PE anti-mouse/human CD45R/B220, clone RA3-6B2, dilution 1:100	BioLegend	Cat# 103208; RRID:AB_312993
Biotin anti-mouse CD197 (CCR7), clone 4B12, dilution 1:50	BioLegend	Cat# 120104; RRID:AB_389232
FITC anti-human Ig light chain κ, clone MHK-49, dilution 1:100	BioLegend	Cat# 316506; RRID:AB_493611
Biotin anti-human Ig light chain κ, clone MHK-49, dilution 1:100	BioLegend	Cat# 316504; RRID:AB_493609
PE anti-mouse Nur77, clone 12.14, dilution 1:100	eBioscience	Cat# 12-5965-82; RRID:AB_1257209
PE anti-mouse CD69, clone H1.2F3, dilution 1:100	eBioscience	Cat# 12-0691-82; RRID:AB_465732
APC anti-mouse CD64, clone X54-5/7.1, dilution 1:100	BioLegend	Cat# 139306; RRID:AB_11219391
Alexa Fluor 647 anti-mouse CD31, clone MEC13.3, dilution 1:100	BioLegend	Cat# 102516; RRID:AB_2161029
Brilliant Violet 421 anti-mouse F4/80, clone BM8, dilution 1:100	BioLegend	Cat# 123132; RRID:AB_10901171
PE anti-mouse IFN-γ, clone XMG1.2, dilution 1:100	BioLegend	Cat# 12-7311-82; RRID: AB_466193
APC anti-mouse MHC Class I (H-2K^{b}), clone AF6-88.5.5.3, dilution 1:100	eBioscience	Cat# 17-5958-82; RRID:AB_1311280

Super Bright 436 anti-mouse MHC Class I (H-2K^{d}), clone SF1-1.1.1, dilution 1:100	eBioscience	Cat# 62-5957-82; RRID:AB_2744812
PE anti-mouse H-2K^{b} bound to SIINFEKL, clone 25-D1.16, dilution 1:100	BioLegend	Cat# 141604; RRID:AB_10895905
Alexa Fluor 700 anti-mouse CD3, clone 17A2, dilution 1:100	BioLegend	Cat# 100216; RRID:AB_493697
Biotin anti-mouse CD3 antibody, clone 17A2, dilution 1:100	BioLegend	Cat# 100244; RRID:AB_2563947
APC Hamster anti-mouse CD3e, clone 145-2C11, dilution 1:100	BD Biosciences	Cat# 553066; RRID:AB_398529
Super Bright 436 anti-mouse CD45R (B220), clone RA3-6B2, dilution 1:100	eBioscience	Cat# 62-0452-82; RRID:AB_2734992
Alexa Fluor 647 anti-mouse CD45.1, clone A20, dilution 1:100	BioLegend	Cat# 110720; RRID:AB_492864
FITC anti-mouse IgD, clone 11-26c, dilution 1:100	eBioscience	Cat# 11-5993-85; RRID:AB_465347
APC anti-mouse CD45.2, clone 104, dilution 1:100	BioLegend	Cat# 109814; RRID:AB_389211
Rabbit anti Hepatitis B Surface Antigen, Polyclonal, dilution 1:100	Bio-Rad	Cat# OBT0990; RRID:AB_609657
Peroxidase AffiniPure Donkey anti-Rabbit IgG (H+L), dilution 1:200	Jackson ImmunoResearch Labs	Cat# 711-035-152; RRID:AB_10015282
Peroxidase-AffiniPure Goat anti-Mouse IgG (H+L), dilution 1:10000	Jackson ImmunoResearch Labs	Cat# 115-035-003; RRID:AB_10015289
Peroxidase IgG Fraction Monoclonal mouse anti-Fluorescein (FITC), dilution 1:200	Jackson ImmunoResearch Labs	Cat# 200-032-037; RRID:AB_2314402
Alkaline Phosphatase Streptavidin, dilution 1:200	Jackson ImmunoResearch Labs	Cat# 016-050-084; RRID:AB_2337239
Alexa Fluor 488 IgG Fraction Monoclonal mouse anti-Fluorescein (FITC), dilution 1:200	Jackson ImmunoResearch Labs	Cat# 200-542-037; RRID:AB_2339038
Cy3 IgG Fraction Monoclonal mouse anti-biotin, dilution 1:200	Jackson ImmunoResearch Labs	Cat# 200-162-211; RRID:AB_2339026
Alexa Fluor 647 anti-mouse DC Marker (33D1), clone 33D1, dilution 1:100	BioLegend	Cat# 124912;RRID:AB_1227623

Alexa Fluor 647 goat anti-rabbit IgG (H+L) Highly Cross-Adsorbed Secondary Antibody, dilution 1:100	ThermoFisher Scientific	Cat# A-21245; RRID:AB_2535813
InVivoMAb anti-mouse L-Selectin (CD62L), clone Mel-14	BioXCell	Cat# BE0021; RRID:AB_1107665
InVivoMAb anti-mouse LFA-1α (CD11a), clone M17/4	BioXCell	Cat# BE0006; RRID:AB_1107578
InVivoMAb anti-mouse/human VLA-4 (CD49d), clone PS/2	BioXCell	Cat# BE0071; RRID:AB_1107657
InVivoMAb anti-mouse CD4, clone GK1.5	BioXCell	Cat# BE0003-1; RRID:AB_1107636
InVivoMAb anti-mouse ICOS, clone 7E.17G9	BioXCell	Cat# BE0059; RRID:AB_1107622
InVivoMAb anti-mouse CLEC9A (CD370), clone 7H11	BioXCell	Cat# BE0305; RRID:AB_2721034
Mouse XCL1/Lymphotactin Antibody, clone 80222	R&D Systems	Cat# MAB486; RRID:AB_2216913
H-2K^{b}-ENV353 (VWLSVIWM) tetramer, dilution 1:50	MBL life science	Cat# TC-5110-1
Anti-idiotypic antibody 35.6, dilution 1:100	European Virus Archive Global	N/A
TotalSeq-B0303 anti-mouse Hashtag 3	BioLegend	Cat# 155835; RRID:AB_2814069
TotalSeq-B0304 anti-mouse Hashtag 4	BioLegend	Cat# 155837; RRID:AB_2814070
TotalSeq-C0251 anti-human Hashtag 1	BioLegend	Cat# 394661; RRID:AB_2801031
TotalSeq-C0252 anti-human Hashtag 2	BioLegend	Cat# 394663; RRID:AB_2801032
TotalSeq-C0253 anti-human Hashtag 3	BioLegend	Cat# 394665; RRID:AB_2801033

Supplememtary Table 2. List of reagents or resources used in this study.

REAGENT or RESOURCE	SOURCE	IDENTIFIER
Chemicals, peptides, and recombinant proteins		
APC Streptavidin, dilution 1:200	BioLegend	Cat# 405207
Streptavidin Super Bright 600 Conjugate, dilution 1:200	eBioscience	Cat# 63-4317-82
Fetal Bovine Serum	Biological industry	Cat# 04-001
Penicillin-streptomycin	Thermo Fisher Scientific	Cat#15070-063
L-Glutamine	Corning	Cat# 25-005-CI
Dulbecco's Phosphate Buffered Saline	Biological industry	Cat# 02-023-1A
Hematoxylin Staining Solution	Beyotime	Cat# C0107
Permanent Aqueous Mounting Medium	Bio-Rad	Cat# BUF058B
Maraviroc (UK-427857)	Selleck	Cat# S2003
CTLA4-Ig	ZXBio	Cat# ZXRU015-N2
Tamoxifen	Sigma Aldrich	Cat# 85256
Mouse recombinant CD6 Protein (hFc Tag)	SinoBiological	Cat# 50711-M02H
Fixable Viability Dye eFluor 780	eBioscience	Cat# 65-0865-18
Diphtheria Toxin, unnicked, from *Corynebacterium diphtheriae*	list labs	Cat# 150
Percoll	GE Healthcare	Cat# GE17089109
Collagenase, Type 4	Worthington	Cat# LS004186
Deoxyribonuclease I from bovine pancreas	Sigma Aldrich	Cat# DN25
Bovine Serum Albumin	Sigma Aldrich	Cat# A2153
Clodronate Liposomes (Anionic)	FormuMax Scientific	Cat# F70101C-A-2
Proteinase K	YEASEN	Cat# 10401ES80
Brefeldin A	Selleck	Cat# S7046
Recombinant Hepatitis B virus surface antigen	Bioforce	Cat# HB-004
16% Formaldehyde (w/v), Methanol-free	Thermo Fisher Scientific	Cat# 28908
3-Amino-9-ethylcarbazole	Sigma Aldrich	Cat# A5754
Naphthol AS-MX phosphate	Sigma Aldrich	Cat# N4875
DAPI, FluoroPure grade	ThermoFisher Scientific	Cat# D21490
Phosphatase substrate	Sigma Aldrich	Cat# S0942
N, N-Dimethylformamide	Sigma Aldrich	Cat# D4551
3, 3′-Diaminobenzidine	Sigma Aldrich	Cat# D8001
Fast Blue BB Salt hemi (zinc chloride) salt	Sigma Aldrich	Cat# 44670
Critical commercial assays		
MojoSort Mouse CD8 T Cell Isolation Kit	BioLegend	Cat# 480035
MojoSort Mouse CD4 T Cell Isolation Kit	BioLegend	Cat# 480033

MojoSort Mouse CD45.1 Selection Kit	BioLegend	Cat# 480118
EasySep Mouse B Cell Isolation Kit	Stemcell	Cat# 19854
NucleoBond Xtra Midi EF	Macherey-Nagel	Cat# 740420.50
IC Fixation Buffer	eBioscience	Cat# 00-8222-49
Foxp3 / Transcription Factor Staining Buffer Set	eBioscience	Cat# 00-5523-00
TSA™Biotin System	PerkinElmer	Cat# NEL700A001KT
CellTrace Violet Cell Proliferation Kit	Thermo Fisher Scientific	Cat# C34557
Cell Stimulation Cocktail (plus protein transport inhibitors) (500X)	Thermo Fisher Scientific	Cat# 00-4975-03
HBsAg ELISA Kit	Shanghai Kehua Bio-Engineering Co.	Cat# KH-T-01*
HBsAg CLIA Kit	Autobio Diagnostics Co.	Cat# CL0310-2
Alexa Fluor 647 Antibody Labeling kit	Thermo Fisher Scientific	Cat# A20186
EZ-Link Sulfo-NHS-SS-Biotin	Thermo Fisher Scientific	Cat# 21331
MojoSort Streptavidin Nanobeads	BioLegend	Cat# 480016
Chromium Next GEM Single Cell 3' GEM, Library & Gel Bead Kit v3.1	10x Genomics	Cat# 1000121
Chromium Single Cell 3' Feature Barcode Library Kit	10x Genomics	Cat# 1000079
Chromium Next GEM Chip G Single Cell Kit	10x Genomics	Cat# 1000120
Chromium Next GEM Single Cell 5' Kit v2	10x Genomics	Cat# 1000263
Library Construction Kit	10x Genomics	Cat# 1000190
5' Feature Barcode Kit	10x Genomics	Cat# 1000256
Chromium Single Cell Human TCR Amplification Kit	10x Genomics	Cat# 1000252
Chromium Single Cell Human BCR Amplification Kit	10x Genomics	Cat# 1000253
Chromium Single Cell Mouse TCR Amplification Kit	10x Genomics	Cat# 1000254
Chromium Next GEM Chip K Single Cell Kit	10x Genomics	Cat# 1000286